Mid-infrared absorption spectroscopy and differential damage *in vitro* between lipids and proteins by an all-fiber-integrated supercontinuum laser

Kevin Ke,[1] Chenan Xia, [1] Mohammed N. Islam, [1,3*] Michael J. Welsh, [2] and Michael J. Freeman[3]

[1]*Department of Electrical Engineering and Computer Science, University of Michigan, 1301 Beal Avenue, Ann Arbor, Michigan 48109*
[2]*Department of Cell and Developmental Biology, University of Michigan, 109 Zina Pitcher Place, Ann Arbor, Michigan 48109*
[3]*Omni Sciences Inc., 647 Spring Valley Drive, Ann Arbor, Michigan 48105*
**mni@eecs.umich.edu*

Abstract: We identify and differentially damage lipids and proteins using wavelengths between 2.6 and 3.8 μm from a fiber-based supercontinuum (SC) laser. Absorption spectroscopy of the constituents of normal artery and atherosclerotic plaque, including adipose tissue, macrophages and foam cells, are measured by a SC laser in the mid-infrared. By using the laser light within the C-H fatty acid and cholesterol esters absorption band, we also demonstrate differential damage of lipid-rich adipose tissue without damaging the protein-rich blood vessel wall. The experiments use a novel SC laser that is all-fiber-integrated with no moving parts, covers a continuous spectrum ranging from ~0.8 to beyond 4.2 μm, and outputs a time-averaged power scalable up to 10.5 W.

OCIS codes: (320.6629) Supercontinuum generation; (300.6340) Spectroscopy, infrared; (170.1020) Ablation of tissue.

References and links

1. C. Paluszkiewicz, W. M. Kwiatek, A. Banas, A. Kisiel, A. Marcelli, and A. Piccinini, "SR-FTIR spectroscopic preliminary findings of non-cancerous, cancerous, and hyperplastic human prostate tissues," Vib. Spectrosc. **43**(1), 237–242 (2007).
2. H.-Y. N. Holman, K. A. Bjornstad, M. C. Martin, W. R. McKinney, E. A. Blakely, and F. G. Blankenberg, "Mid-infrared reflectivity of experimental atheromas," J. Biomed. Opt. **13**(3), 030503 (2008).
3. K. A. Tillman, R. R. J. Maier, D. T. Reid, and E. D. McNaghten, "Mid-infrared absorption spectroscopy across a 14.4 THz spectral range using a broadband femtosecond optical parametric oscillator," Appl. Phys. Lett. **85**(16), 3366–3368 (2004).
4. E. Sorokin, I. T. Sorokina, J. Mandon, G. Guelachvili, and N. Picqué, "Sensitive multiplex spectroscopy in the molecular fingerprint 2.4 μm region with a Cr2+:ZnSe femtosecond laser," Opt. Express **15**(25), 16540–16545 (2007).
5. M. Razeghi, S. Slivken, Y. Bai, and S. R. Darvish, "The quantum cascade laser: a versatile and powerful tool," Opt. Photonics News **19**(7), 42–47 (2008).
6. J. Mandon, E. Sorokin, I. T. Sorokina, G. Guelachvili, and N. Picqué, "Supercontinua for high-resolution absorption multiplex infrared spectroscopy," Opt. Lett. **33**(3), 285–287 (2008).
7. J. M. Langridge, T. Laurila, R. S. Watt, R. L. Jones, C. F. Kaminski, and J. Hult, "Cavity enhanced absorption spectroscopy of multiple trace gas species using a supercontinuum radiation source," Opt. Express **16**(14), 10178–10188 (2008).
8. C. F. Kaminski, R. S. Watt, A. D. Elder, J. H. Frank, and J. Hult, "Supercontinuum radiation for applications in chemical sensing and microscopy," Appl. Phys. B **92**(3), 367–378 (2008).
9. B. A. Hooper, A. Maheshwari, A. C. Curry, and T. M. Alter, "Catheter for diagnosis and therapy with infrared evanescent waves," Appl. Opt. **42**(16), 3205–3214 (2003).
10. A. P. Joglekar, H. Liu, G. J. Spooner, E. Meyhofer, G. Mourou, and A. J. Hunt, "A study of the deterministic character of optical damage by femtosecond laser pulses and applications to nanomachining," Appl. Phys. B **77**, 25–30 (2003).

#106047 - $15.00 USD Received 6 Jan 2009; revised 11 Jun 2009; accepted 23 Jun 2009; published 10 Jul 2009

11. Y. Xiao, M. Guo, P. Zhang, G. Shanmugam, P. L. Polavarapu, and M. S. Hutson, "Wavelength-dependent conformational changes in collagen after mid-infrared laser ablation of cornea," Biophys. J. **94**(4), 1359–1366 (2008).
12. K. Awazu, A. Nagai, and K. Aizawa, "Selective removal of cholesterol esters in an arteriosclerotic region of blood vessels with a free-electron laser," Lasers Surg. Med. **23**(4), 233–237 (1998).
13. R. R. Anderson, W. Farinelli, H. Laubach, D. Manstein, A. N. Yaroslavsky, J. Gubeli 3rd, K. Jordan, G. R. Neil, M. Shinn, W. Chandler, G. P. Williams, S. V. Benson, D. R. Douglas, and H. F. Dylla, "Selective photothermolysis of lipid-rich tissues: a free electron laser study," Lasers Surg. Med. **38**(10), 913–919 (2006).
14. C. Xia, Z. Xu, M. N. Islam, F. L. Terry, Jr., M. J. Freeman, A. Zakel, and J. Mauricio, "10.5 watts time-averaged power mid-infrared supercontinuum generation extending beyond 4 μm with direct pulse pattern modulation," IEEE J. Sel. Top. Quantum Electron. **15**(2), 422–434 (2009).
15. A. D. Kinkel, M. E. Fernyhough, D. L. Helterline, J. L. Vierck, K. S. Oberg, T. J. Vance, G. J. Hausman, R. A. Hill, M. V. Dodson; A. D., "Oil red-O stains non-adipogenic cells: a precautionary note," Cytotechnology **46**(1), 49–56 (2004).
16. R. A. Neumann, R. M. Knobler, F. Pieczkowski, and W. Gebhart, "Enzyme histochemical analysis of cell viability after argon laser-induced coagulation necrosis of the skin," J. Am. Acad. Dermatol. **25**(6 Pt 1), 991–998 (1991).
17. D. Kritchevsky, "Dietary-protein, cholesterol and atherosclerosis-a review of the early history," J. Nutr. **125**, S589–S593 (1995).
18. T. Arai, K. Mizuno, A. Fujikawa, M. Nakagawa, and M. Kikuchi, "Infrared absorption spectra ranging from 2.5 to 10 microns at various layers of human normal abdominal aorta and fibrofatty atheroma in vitro," Lasers Surg. Med. **10**(4), 357–362 (1990).
19. J. M. Gentner, E. Wentrup-Byrne, P. J. Walker, and M. D. Walsh, "Comparison of fresh and post-mortem human arterial tissue: an analysis using FT-IR microspectroscopy and chemometrics," Cell Mol Biol (Noisy-le-grand) **44**(1), 251–259 (1998).
20. P. Libby, "Atherosclerosis: The new view," Sci. Am. **286**, 47–55 (2002).
21. J. D. Caplan, S. Waxman, R. W. Nesto, and J. E. Muller, "Near-infrared spectroscopy for the detection of vulnerable coronary artery plaques," J. Am. Coll. Cardiol. **47**(8 Suppl), C92–C96 (2006).
22. T. J. Römer, J. F. Brennan 3rd, M. Fitzmaurice, M. L. Feldstein, G. Deinum, J. L. Myles, J. R. Kramer, R. S. Lees, and M. S. Feld, "Histopathology of human coronary atherosclerosis by quantifying its chemical composition with Raman spectroscopy," Circulation **97**(9), 878–885 (1998).
23. P. R. Moreno, B. J. Marshik, and J. E. Muller, "Diffuse reflectance near-infrared spectroscopy as a clinical technique to detect high-risk atherosclerotic plaques," in Handbook of the Vulnerable Plaque, R. Waksman and P. W. Serruys, eds. (Taylor & Francis, 2004), pp. 205–218.
24. L. Wang, J. Chapman, R. A. Palmer, O. van Ramm, and B. Mizaikoff, "Classification of atherosclerotic rabbit aorta samples by mid-infrared spectroscopy using multivariate data analysis," J. Biomed. Opt. **12**, 024006–1-11 (2007).
25. J. M. Isner, D. Gal, P. G. Steg, S. T. DeJesus, A. J. Rongione, K. R. Halaburka, G. A. Slovenkai, and R. H. Clarke, "Percutaneous, in vivo excimer laser angioplasty: results in two experimental animal models," Lasers Surg. Med. **8**(3), 223–232 (1988).
26. G. M. LaMuraglia, S. Murray, R. R. Anderson, and M. R. Prince, "Effect of pulse duration on selective ablation of atherosclerotic plaque by 480- to 490-nanometer laser radiation," Lasers Surg. Med. **8**(1), 18–21 (1988).

1. Introduction

In the mid-infrared (mid-IR) region between 2.6 and 3.8 μm, lipids and proteins have fundamental absorptions that lie at different wavelengths. For the first time to our knowledge, using an all-fiber-integrated supercontinuum (SC) laser, we measure the mid-IR spectral characteristics of biological samples. We acquire the absorption spectra of biological samples, including the constituents of the normal artery and atherosclerotic plaque (AP), in the 2.6-3.8 μm wavelength windows. We observe distinct spectral signatures in 2.8-3.2 μm corresponding to protein and water absorption and in 3.2-3.6 μm that are associated with fatty acids and cholesterol esters. We perform differential damage of lipid-rich tissues by targeting light in the C-H absorption band. Differential damage is possible because proteins show primary light absorption at 2.8-3.2 μm due to N-H and O-H bonds, while lipids exhibit absorptions in 3.2-3.6 μm associated with C-H stretching vibrations. Based on the spectral differentiation, we demonstrate that lipid-rich samples, e.g. adipose tissue, can be differentially damaged without causing damage to normal artery by using a light radiance as low as ~15 mJ/mm^2 in the 3.2-3.6 μm band. Our experiments employ a novel SC laser that provides a continuous spectrum coverage ranging from ~0.8 to 4.2 μm with time-averaged power scalable up to 10.5 W.

The fiber based SC laser source provides a new platform for absorption spectroscopy and tissue damage in the mid-IR. Optical absorption spectroscopy has been widely used to provide the chemical information of biological samples since every molecular vibrational bond resonates at a unique optical frequency [1,2]. Conventionally, thermal lamps, optical

#106047 - $15.00 USD Received 6 Jan 2009; revised 11 Jun 2009; accepted 23 Jun 2009; published 10 Jul 2009

parametric amplifiers [3], broadband femtosecond lasers [4], quantum cascaded lasers [5] and synchrotron lasers [2] are used as the light sources for mid-IR spectroscopic applications. Recently, optical absorption spectroscopy has been reported using SC laser systems in the visible and near infrared (near-IR) wavelength regime. For example, C_2H_2 and NH_3 overtone spectra in the 1.5-1.7 μm region are measured using SC generated in a soft-glass photonic crystal fiber [6]. In addition, various spectral acquisition techniques, including FTIR [6], cavity enhanced absorption spectroscopy [7], and time domain dispersive frequency mapping [8], have been demonstrated to improve the spectral resolution, measurement speed, and signal sensitivity. However, SC based absorption spectroscopy experiments in the mid-IR where the fundamental molecular vibrational modes reside have not yet been reported. In this paper, we demonstrate mid-IR absorption spectroscopy measurements using an all-fiber-integrated SC laser, which has no moving parts, generates the entire spectrum simultaneously in the single spatial mode and operates at room temperature.

Our SC fiber laser can also differentially damage lipid-rich samples by targeting the laser light in the 3.2-3.6 μm fatty acids and cholesterol esters absorption band. While precision damage has been demonstrated using free electron lasers [9] and femtosecond lasers [10], the process is spatially selective but not tissue specific. Single wavelength-dependent selective damage comparing 2.77 μm to 6.45 μm has been performed in collagen for mid-IR laser damage of cornea [11] and 5.75 μm to 6.1 μm for damage of cholesterol esters using free-electron laser [12]. Differential damage of lipid-rich tissue has been also reported by preferentially heating the target fatty tissues above the physiological temperature using lipid absorption bands at 1.21 and 1.72 μm [13]. We show here damages of lipid-rich adipose tissues under conditions that do not damage the normal artery wall in blood vessels. Hence, our SC laser, packaged into a 2U rack unit (19 inches in width/21 inches in depth/4 inches in height), could potentially be deployed in the clinical environment for practical medical use.

This paper is organized as follows. In section 2, we describe the experimental setup and biological sample preparation procedures. In section 3, mid-IR absorption spectroscopy measurements of the constituents of normal artery and atherosclerotic plaque are demonstrated using the SC laser. We present experimental results of differential damage of lipid-rich tissue samples in section 4. Finally, we discuss and summarize the paper in section 5.

2. Experimental setup and sample preparation

The experimental design comprises three parts—the SC laser, mid-IR spectroscopy, and laser damage. The SC laser consists of a 1542 nm distributed feedback (DFB) laser diode, multi-stage fiber amplifiers, and SC generation fibers as illustrated in Fig. 1. The DFB laser outputs seed light with ~0.5 ns pulse width at variable pulse repetition rate. The light is amplified by three stages of fiber amplifiers, in which the first stage is a single mode erbium-doped fiber amplifier and second and third stages are cladding-pumped erbium/ytterbium co-doped fiber amplifiers. Narrow bandpass filters and optical isolators are used in between each amplifier stage to filter out the out-of-band amplified spontaneous emission and minimize back-reflection. The amplified diode pulses are then coupled into a combination of ~2 m length of standard single mode fiber (SMF) followed by ~7 m length of ZBLAN (ZrF_4-BaF_2-LaF_3-AlF_3-NaF) fluoride fiber to generate the SC. The ZBLAN fiber has a core diameter of 8.9 μm, a cladding diameter of 125 μm, and a numerical aperture of 0.20. The output light from the SMF fiber is coupled into the ZBLAN fiber through a mechanical splice.

#106047 - $15.00 USD Received 6 Jan 2009; revised 11 Jun 2009; accepted 23 Jun 2009; published 10 Jul 2009

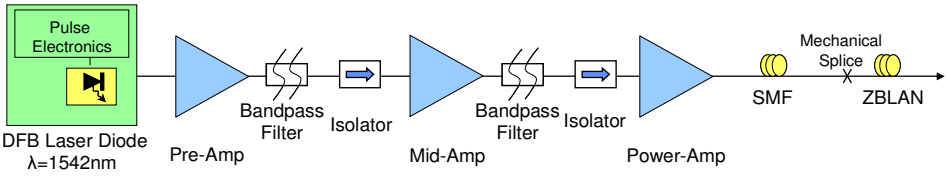

Fig. 1. SC laser setup comprising a DFB laser diode followed by three stages of fiber amplifiers plus SC generation fibers.

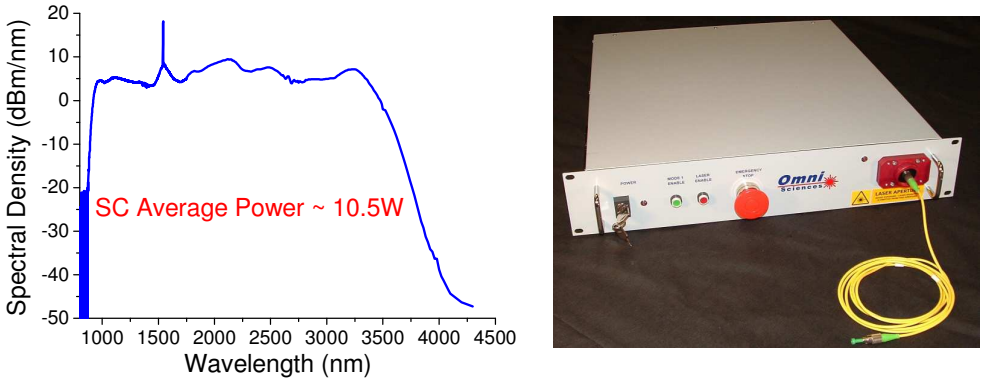

Fig. 2. (a). SC spectrum generated in 2 m length of single mode fibers plus 7 m length of ZBLAN fibers (left). (b). Illustration of 2.5 W mid-IR SC laser prototype (inside follows the block diagram of Fig. 1) (right).

As illustrated in Fig. 2 (a), the SC laser provides a spectrum coverage extending from ~0.8 μm to 4 μm with a time-averaged output power scalable up to 10.5 W. All of the spectral components of the SC output are generated simultaneously and in single spatial mode. It should be noted that although the SC laser has been demonstrated with up to 10.5 W average output power, the spectroscopy measurements and laser damage are conducted with only a few of the pump laser diodes on and ~1.5 W SC output power. Further details of the SC laser are described in [14]. Also, to illustrate that our SC laser can be made compact for potential clinical applications, Fig. 2(b) shows a picture of a 2.5 W output power prototype laser corresponding to the optical block diagram of Fig. 1. This is a 2U rack unit (19 inches in width/21 inches in depth/4 inches in height) that plugs into the wall and has a serial port for computer controlled laser pulse pattern modulation.

For absorption spectrum measurements, the output of the SC laser is coupled to the mid-IR spectroscopy setup shown in Fig. 3(a). We use a parabolic off-axis mirror to collimate the SC light and to minimize the chromatic aberration. To improve the signal-to-noise ratio of the measurements, a 50/50 CaF_2 based beam splitter splits the collimated SC output into two beams, i.e. one signal arm and one reference arm, which are modulated by optical choppers at different frequencies. The light of the signal arm is focused by a 25.4 mm focal length CaF_2 lens onto the sample placed on a mid-IR reflective substrate, e.g. gold coated slide or MirrIR microscope slide (Kevley Technologies, Chesterland, OH). The reflected light is then re-collimated by the same lens and recombined with the reference arm by another 50/50 beam splitter. The recombined SC light is coupled into a grating-based spectrometer with signal collected by a liquid-nitrogen cooled InSb detector. A 2500 nm long pass filter is placed in the optical path to remove the higher-order diffractions of the SC spectrum in the spectrometer, and optical apertures are used to obtain the optimal signal strength for both arms. The signal from the detector is acquired by two lock-in amplifiers with each synchronized to its respective optical chopper. The amplitude fluctuation of the SC laser is compensated for by

#106047 - $15.00 USD Received 6 Jan 2009; revised 11 Jun 2009; accepted 23 Jun 2009; published 10 Jul 2009

taking the ratio of the two arms. Therefore, the mid-IR spectroscopy system is able to detect a change of the SC spectral amplitude within less than 1%. As illustrated in Fig. 3(b), the corrected SC amplitude fluctuation after taking the ratio of sample beam signal over reference is within 0.7% at 3400 nm for 400 s.

For the differential damage experiment, the SC laser is used in conjunction with the damage set-up of Fig. 3(c). The SC light residing in the lipids vibrational bands is selected out by a ~3200 nm long pass filter. For the damage experiments, the laser pulse width is set to 1 ns and the shape of the SC spectrum is maintained for different power levels. The collimated SC beam diameter is estimated to be ~9 mm. The filtered light is then focused by a 25.4 mm CaF_2 lens to a spot size of ~3 mm onto the sample. Substrates holding thin samples are made of mid-IR transparent materials, e.g. CaF_2 or KCl window (International Crystal Laboratories, Garfield, NJ), to reduce the substrate-absorption induced heating effects.

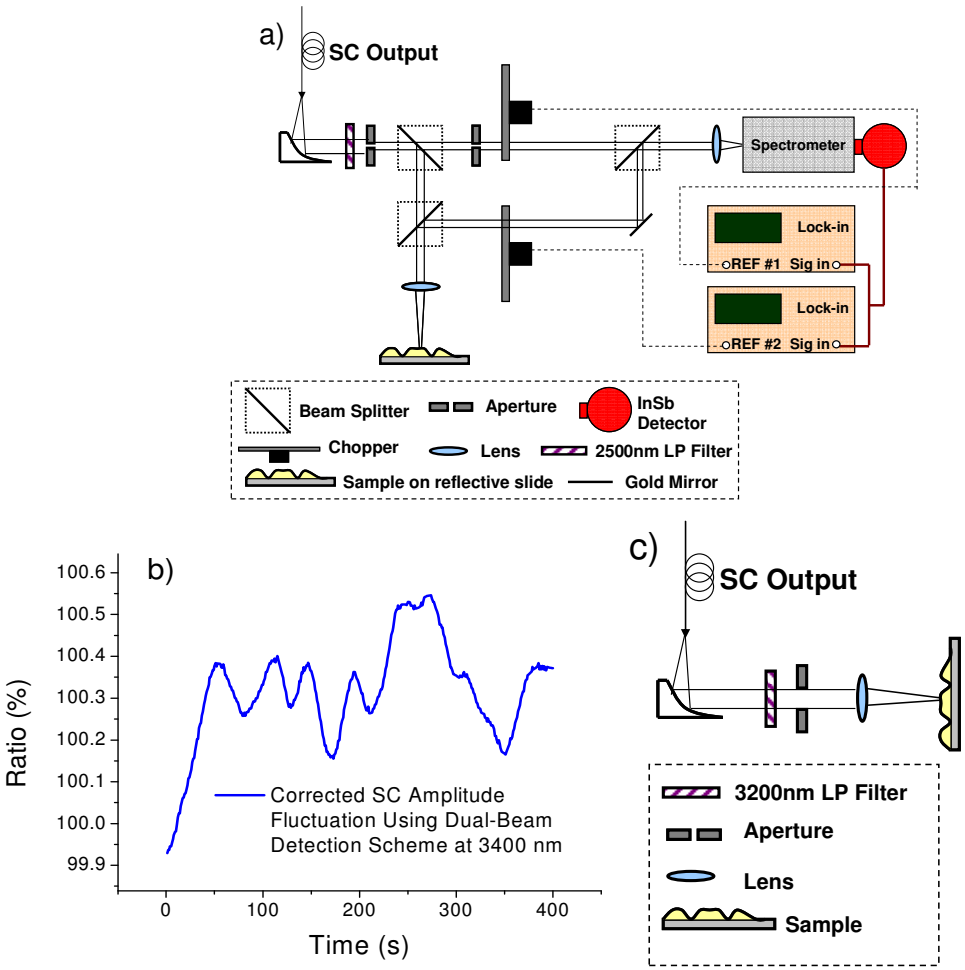

Fig. 3. Experimental setup for (a) reflection-absorption spectra measurement, (b) measured SC amplitude fluctuation using dual-beam detection scheme at 3400 nm, and (c) differential laser damage.

SC based spectroscopy experiments were performed *in vitro* on cultured cells and dried egg yolk powder (Sigma-Aldrich, Milwaukee, WI). Cells were grown using the following methodology. Endothelial cells and smooth muscle cells were cultured for 24 hours in RPMI medium containing antibiotics (streptomycin and penicillin, Gibco) and 10% fetal bovine serum. Murine macrophages (cell line J774A.1) were plated onto 2.5 cm square pieces of MirrIR microscope slides (Kevley Technologies). To improve adherence of the cells to the

#106047 - $15.00 USD Received 6 Jan 2009; revised 11 Jun 2009; accepted 23 Jun 2009; published 10 Jul 2009

glass slide substrate, the glass had been previously incubated for 20 minutes in a 100µg/ml solution of poly-L-lysine (Sigma Chem., #P-1399) in sterile water. The poly-L-lysine solution was removed and the glass was air dried for 2 hours. Sterility of the glass substrates was achieved by exposing each side of the glass to a germicidal UV lamp for 20 minutes. Macrophages were then plated onto the glass substrates at high cell density to achieve total coverage of the substrate by the cells. Macrophages were cultured for 24 hours in RPMI medium containing antibiotics (streptomycin and penicillin, Gibco) and 10% fetal bovine serum. Macrophages were then activated by treatment with 1 µg/ml lipopolysaccharide (LPS from *Salmonella minnesota* R595, Axxora, San Diego, CA) for 24 hours. At this point, macrophages were treated with the cholesterol/PC liposomes for 48 hours to generate foam cells, and then the cells were used for experiments.

Liposomes were made as follows: 25 mg each of cholesterol (Sigma-Aldrich, Milwaukee, WI) and egg phosphatidylcholine (PC, Sigma-Aldrich) were dissolved in 1 ml of chloroform in a 15 x 125 mm glass tube. The chloroform was evaporated leaving the cholesterol/PC as a residue on the surface of the glass tube. 7 ml of RPMI 1640 culture medium (Invitrogen/Gibco, Carlsbad, CA) containing 10% fetal calf serum (Invitrogen/Gibco) was added to the tube and liposomes were made by sonicating the cholesterol/PC mixture in the culture medium using a Tekmar TM40 sonic disruptor set to maximum output for one minute. This suspension was then passed through a 0.45 micrometer pore size sterile filter.

To observe lipids within foam cells, cells were prepared in a manner similar to that described by Kinkel *et al*. [15]. Cells were fixed with 4% formaldehyde solution for 1 hour, rinsed in phosphate buffered saline and then rinsed with 2 changes of ethylene glycol for 2 minutes each. Cells were then incubated in a solution of oil red O in ethylene glycol for 20 minutes, rinsed twice for 5 minutes each in ethylene glycol and then rinsed in water. Macrophages exhibited no oil red O staining droplets while LPS activated/liposome fed macrophages (foam cells) exhibited numerous lipid droplets (Fig. 4).

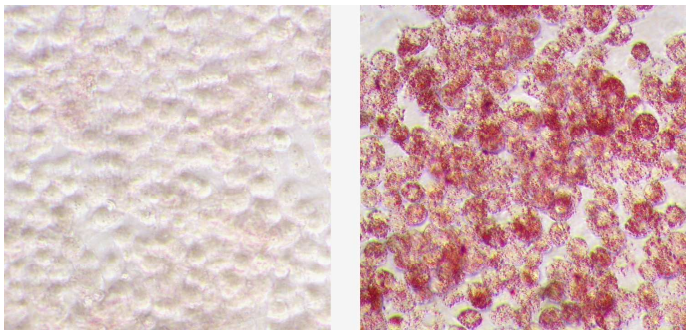

Fig. 4. Microscope images of macrophages (left) and foam cells (right). Both cell preparations are stained with oil red O. Macrophages contain essentially no lipid droplets while macrophages differentiated into foam cells (right) exhibit numerous lipid droplets.

We also use Perkin-Elmer Spectrum BX FTIR to measure the relative absorption strengths of different biological tissues. Bovine tissue samples of adipose, aorta, coronary artery, and heart muscle were obtained immediately after the animals were butchered. The animals were healthy and the artery tissues did not contain signs of atheromatic lesion. Tissues were cut to 1 cm by 1 cm squares, 2 to 3 mm in thickness, and flash frozen with liquid nitrogen to prevent water crystal formation. The tissues were then embedded with OCT embedding compound and the temperature was allowed to rise to about −25 degree Celsius inside a Leica CM1850 Cryostat. Upon reaching this temperature, the tissues were cryotome sectioned to 7 micrometer in thickness and laid flat against and covering most of the 15mm aperture of KCl IR card (International Crystal Laboratories, Garfield, NJ). These prepared optical specimens were kept on ice to prevent dehydration when transporting to the FTIR facility. FTIR spectroscopy was performed using a Perkin-Elmer Spectrum BX at 0.5 cm^{-1} resolution, averaged across 8 scans. The wave-number units in the absorption spectra were then

#106047 - $15.00 USD Received 6 Jan 2009; revised 11 Jun 2009; accepted 23 Jun 2009; published 10 Jul 2009

converted into wavelength units. During FTIR spectroscopy, no provision was made to prevent tissue from dehydrating. As a result each subsequent scan showed decreased water absorption. However, all samples should have experience roughly similar dehydration.

In laser damage experiments, tissue samples were cut to about 1.5 cm by 1.5 cm squares, 2 to 3 mm in thickness and flattened with the back of the tissue piece against a piece of glass slide. Laser focus on the surface of the sample was determined by measuring the spot size obtained by a CCD camera and adjusted to lower the laser intensity if required by moving past the laser focus. However, to ease data interpretation, all damages in the same experiment are performed at the same distance from the laser focus. For the experiments comparing the damage threshold of adipose and artery tissue, the samples did not undergo a drying process. These experiments typically took less than 1 hour. Immediately after the laser experiment, the tissue samples are placed in 3.5% formaldehyde in PBS, pH 7.4. After dehydration with a series of increased concentration of alcohol and then xylene, the specimens were embedded in paraffin and sectioned to 7 μm. Tissue sections were affixed to glass microscope slides and stained with hematoxylin and eosin (H&E). Tissue sections were examined by bright field and polarized light microscopy

For the data presented in Fig. 10, a slightly different procedure was followed in order to ease histology preparation. In these experiments, tissue samples were cut to about 1.5 cm by 3 cm, 5 mm in thickness and flattened with the back of the tissue piece against a Styrofoam plate then mounted on a piece of glass slide. The laser beam was collimated at about 2.7mm in diameter and scanned across the tissue surface at 1 cm/minute. Immediately after the laser experiment, the tissue samples were cut into two pieces with a razor blade. One piece of this tissue was placed in 3.5% formaldehyde in PBS, pH 7.4 for H&E and polarized light histological examination was conducted as previously described. The other piece of tissue was embedded in O.C.T (Optimal Cutting Temperature Compound, Tissue-Tek) and placed in liquid nitrogen for cryo-histological examination using MTT (Thiazolyl Blue Tetrazolium Bromide, Sigma-Aldrich) staining. After the temperature of the sample settled around −20°C, the sample was cut into 10 μm -thin slices and stained with MTT following the protocol described in Neumann *et al*. [16]. Briefly, a histochemical solution was prepared by mixing 2.5 ml MMT at 2.0 mg/ml distilled water, 1.0 ml of β-NADH (Sigma-Aldrich) in 2.5 mg/ml distilled water, 1.0 ml phosphate-buffered saline, and 0.5 ml Ringer's solution. Tissue slices were incubated in the solution for 15 minutes under aerobic conditions at room temperature and in the absent of light.

3. Mid-infrared spectroscopy of biological samples

Mid-IR absorption spectra of the components of normal artery, which includes endothelial cells and smooth muscle cells, are illustrated in Fig. 5(a) and (b). As the compositional elements of the normal artery, endothelial cells and smooth muscle cells exhibit similar absorption features in the 2.6-3.8 μm wavelength range. A broad absorption feature ranging from 2.8 to 3.2 μm and peaking at ~3050 nm is observed, and can be attributed to the vibrational bands of O-H stretching in the hydroxyl group and N-H stretching present in the protein amino acids [1,2].

#106047 - $15.00 USD Received 6 Jan 2009; revised 11 Jun 2009; accepted 23 Jun 2009; published 10 Jul 2009

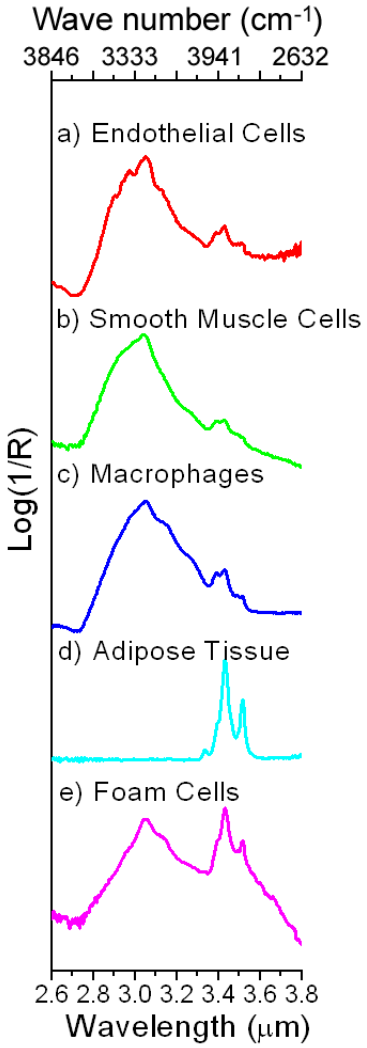

Fig. 5. Mid-IR SC laser based reflection-absorption spectra of normal artery compositions: a) endothelial cells, b) smooth muscle cells; and atherosclerotic plaque constituents: c) macrophages, d) adipose tissue, e) foam cells.

The absorption spectra for the constituents of AP, including macrophages, adipose tissue, and foam cells are illustrated in Fig. 5(c), (d) and (e). In the lipid-rich samples, including adipose tissue and foam cells, we are able to distinguish the individual absorption lines in the 3.2-3.6 μm windows, e.g. = CH stretching vibration at ~3330 nm, CH_3 stretching vibration at ~3390 nm, and CH_2 stretching vibration at ~3420 nm and ~3510 nm [1]. In addition, while the macrophages exhibit a similar absorption spectrum as compared to the normal artery cells, prominent spectral characters between ~3.2 to 3.6 μm with two absorption peaks at ~3420 nm and ~3510 nm are observed in the macrophages-transformed foam cells and adipose tissue absorption spectra. Such spectral pattern arises from the absorptions of hydrocarbon chains, e.g. CH_2 and CH_3 bonds, present in both the fatty acids and cholesterol esters [2]. Therefore, the spectral difference between the macrophages and foam cells is consistent with the pathological relationship between these two cell types, i.e. macrophages engulf lipid-rich substances to become foam cells.

#106047 - $15.00 USD Received 6 Jan 2009; revised 11 Jun 2009; accepted 23 Jun 2009; published 10 Jul 2009

To further investigate the composition properties of the constituents of AP, we measured the absorption spectrum of egg yolk, which is considered to be a conventional composite model of atherogenic lipoprotein [17]. The spectral character of egg yolk (Fig. 6), shares many similarities with that of foam cells (see Fig. 5(e)). Compared to endothelial cells and smooth muscle cells, which form the normal artery, egg yolk shows clear lipid-rich absorption features in 3.2-3.6 μm wavelength range while having comparable absorptions in the 2.8-3.2 μm O-H and N-H vibrational bands. More detailed physical modeling and spectroscopic study of the atherosclerotic tissues have also been conducted by other groups [2,9,18].

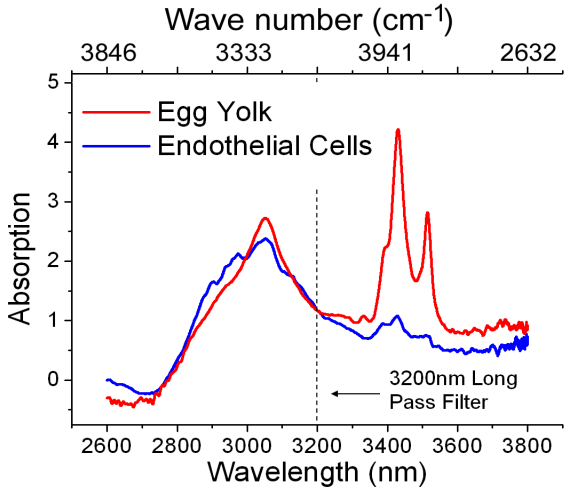

Fig. 6. Mid-IR SC laser based reflection-absorption spectra of a) egg yolk, b) endothelial cells. The two spectra are plotted in logarithm scale and the absorption spectra are vertically displaced to match the absorption feature around 3 μm.

4. Differential damage of lipid-rich tissues

Differential damage takes advantage of the differential absorption of different tissues. In other words, the targeted tissue is preferentially heated to a temperature lethal to cells by laser radiation within the corresponding signature absorption band. Figure 7 illustrates the relative absorption spectra of adipose tissue in comparison with arteries and heart muscle using FTIR spectroscopy. All the samples were prepared by microtome techniques to have a uniform thickness of ~7 μm as explained earlier. We observe that the adipose tissue demonstrates dominant absorption peaks associated with the fatty acids in the 3.2-3.6 μm window compared to artery and muscle components. The measurements confirm that the lipid-rich tissues are prone to absorbing more light in the 3.2-3.6 μm spectral region. It should be noted that the variation of the sample thicknesses is estimated to be ~2 μm, which may contribute to the difference of the baseline absorbance around 2.5 μm. Therefore, we hypothesize, by blocking the common absorption band with a 3.2 μm long wavelength pass filter, that adipose tissue could be preferentially heated by the SC laser pulse through the tissue specific absorption band in 3.2-3.6 μm.

#106047 - $15.00 USD Received 6 Jan 2009; revised 11 Jun 2009; accepted 23 Jun 2009; published 10 Jul 2009

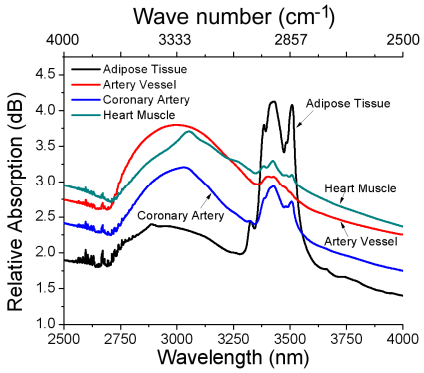

Fig. 7. Absorption spectra measured by FTIR of a) adipose tissue, b) artery vessel, c) coronary artery, and d) heart muscle. The thickness of the samples is 7 μm +/– 2 μm. The spectra are plotted in logarithm scale.

We accomplished differential damage of adipose tissue in comparison to artery wall (Fig. 8) using the SC laser. Each spot of the sample is exposed under the filtered SC light (3.2-3.6 μm) for 5 s with an estimated beam focal spot size of ~3 mm. Differential damage, i.e. preferential heating (or thermal modification) of adipose tissue without damaging artery tissue, is observed under light microscopy with a SC laser fluence starting as low as ~15 mJ/mm^2. On the other hand, we cannot identify any surface damage or colorization in the artery sample over the entire range of ~10-100 mJ/mm^2. For example, a laser fluence of ~33 mJ/mm^2 is calculated by using an incident laser power of ~47 mW, an exposure time of 5 s and a beam diameter of ~3 mm. Figure 8(b) shows the surface morphological difference between adipose tissue and bovine artery at power levels around ~40 mJ/mm^2 using light microscope images, which exhibit thermal damage in adipose tissue but no visible surface damage in bovine artery.

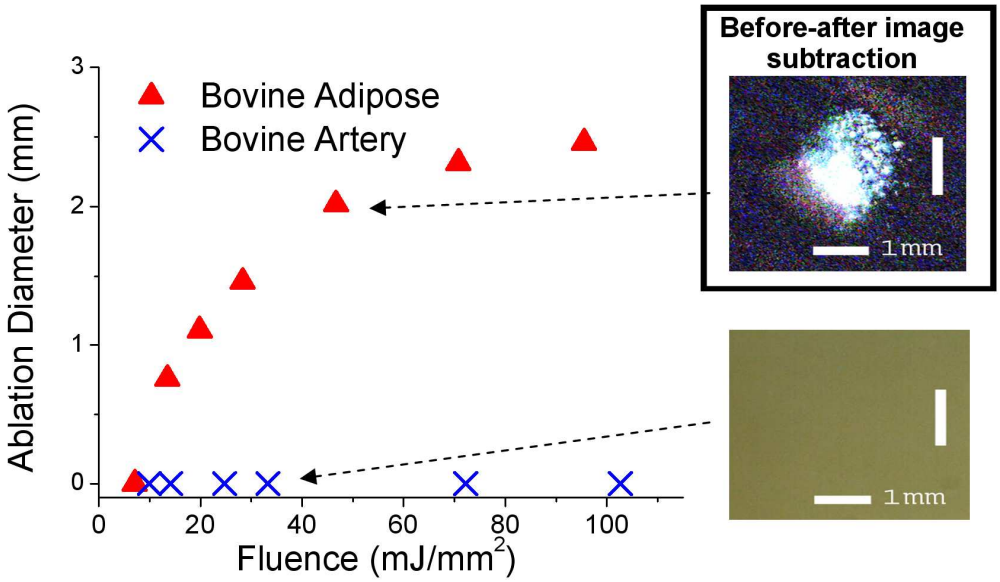

Fig. 8. Differential damage of adipose tissue: a) power dependence of the damage diameter in adipose tissue and bovine artery, b) tissue image after damage at different laser fluence levels. Laser pulse duration is 1 ns, and exposure time is 5 s. The repetition rate of the laser pulse varies from ~100 kHz to 500 kHz depending on fluence level. The adipose tissue image is a subtraction of before and after laser damage; the damaged region is in bright color while the unaffected region is dark color.

#106047 - $15.00 USD Received 6 Jan 2009; revised 11 Jun 2009; accepted 23 Jun 2009; published 10 Jul 2009

To further confirm our hypothesis, we conducted cross section histology to study the biological integrity and possible subsurface damage to bovine artery. Histological sections were prepared according to the procedures presented in Section 2. The criteria for identifying damaged region in H&E and birefringence histology sections are based on discoloration, change in tissue texture, and depression of the cellular and extracellular components. The depression of tissue becomes visible to the naked eye after leaving the tissue in formalin for about 1 hour so it does not appear to be caused by histological preparation. The criterion for identifying damaged region in MTT histology sections are based on the lack of blue stain. Figure 9(a) shows the H&E stained cross section histology of the artery tissue at different laser power levels. While laser induced damage can be observed at a laser fluence of ~102 mJ/mm^2, very subtle effects exist at ~72 mJ/mm^2, and no effect was seen at ~33 mJ/mm^2. We also observe the same slides under polarized light to detect birefringence of collagen. We observe some loss of birefringence, which corresponds to the denaturing of the collagen, at ~102 mJ/mm^2, but no changes in birefringence could be detected at laser fluence of ~72 mJ/mm^2 and ~33 mJ/mm^2 (Fig. 9(b)). The H&E and birefringence results are consistent because collagen typically has a higher thermal tolerance than other artery tissue components, e.g. endothelium and smooth muscle cells. MTT results also appear to agree with H&E and birefringence results in that there is only minimal damage at 80 mJ/mm^2.

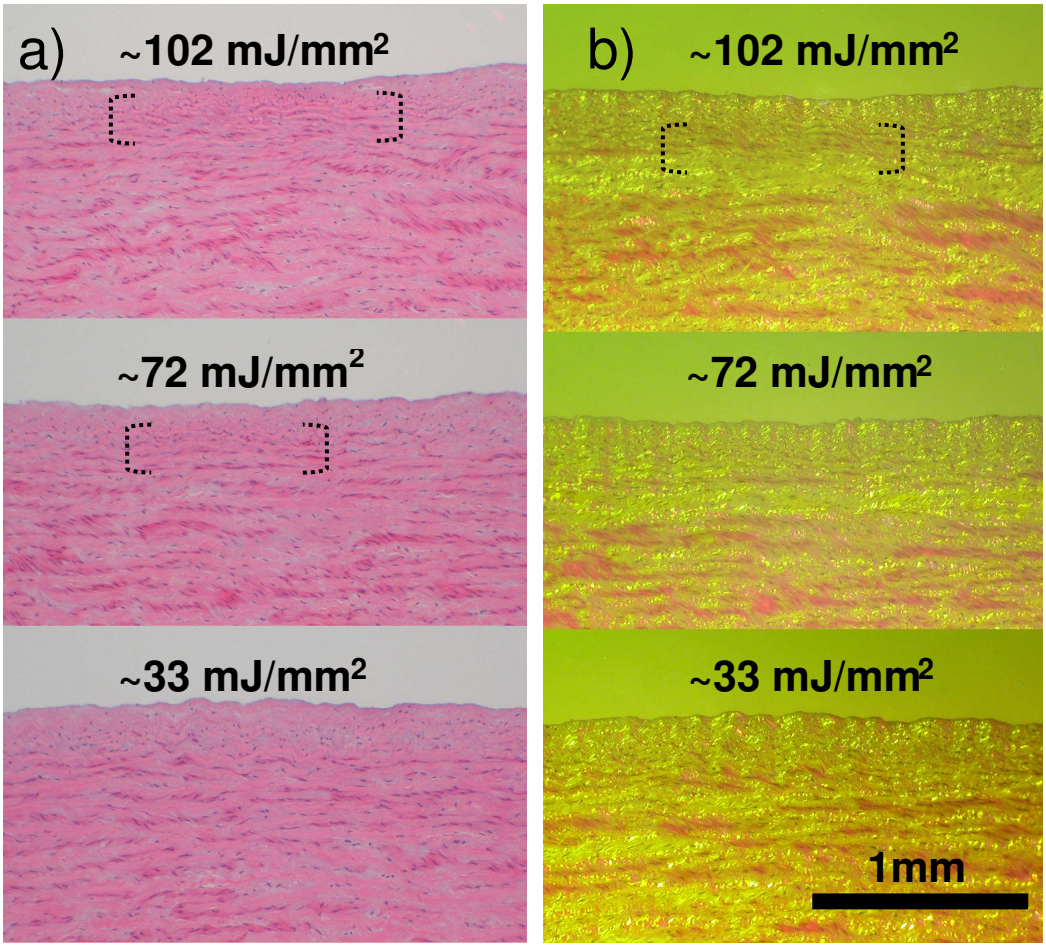

Fig. 9. Histology of artery tissue at different laser fluence levels: a) H&E stained, b) birefringence imaging. Areas of laser effect are indicated by dotted line brackets.

#106047 - $15.00 USD Received 6 Jan 2009; revised 11 Jun 2009; accepted 23 Jun 2009; published 10 Jul 2009

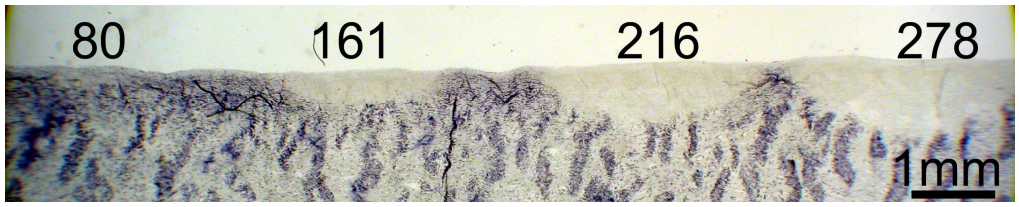

Fig. 10. MTT staining of artery tissue at laser fluence of 80, 161, 216, and 278 mJ/mm^2. Laser damaged region lacks MTT stains.

5. Discussion

Our SC laser can serve as the light source for mid-IR spectroscopy measurements. Using the mid-IR SC laser, we show that the spectral fingerprinting and absorption spectroscopy data is consistent with previously reported data in the 2.5-4 μm wavelength range that is obtained using either a traditional lamp-based or a synchrotron laser-based FTIR measurement system [2,9,19]. Compared to the low signal power available in the lamp-based system and the complex setup of the synchrotron laser, the all-fiber-integrated light source has no moving parts, operates at room temperature, and can be scaled up in time-averaged power to exceed 10 W [14]. Our SC laser based spectroscopy system is able to reveal the subtle spectral difference between different biological samples with adequate signal-to-noise ratio. The results are consistent with the chemical composition of the biological samples, where the C-H stretching bonds present in the lipid-rich tissues give rise to the absorption band in 3.2-3.6 μm, while N-H and O-H bonds dominant in the normal artery tissue absorb light in the 2.8-3.2 μm region [2]. We measure the absorption spectra by using a SC average power of <1 mW and scale up the power to the range of 20-200 mW (~10-100 mJ/mm^2) for damage experiments. In addition, while optical microscopy is sufficient to track damage to adipose tissue, histological staining is required to reveal the very subtle damage in artery tissue. We observe subtle changes in H&E and MTT staining at lower laser fluence than we could find any decreases in the collagen birefringence, which indicates that loss of birefringence is not a sensitive, simple method for detecting tissue damage.

Our spectroscopic results indicate that fat tissue would absorb more energy in the 3.2-3.6 μm window. This was confirmed by irradiating adipose and artery tissues, where greater effect was seen in adipose tissue at laser fluences that caused no visible effect in artery. Changes in collagen birefringence were previously used as a marker for free electron laser-induced damage to tissues [13]. Our results of mid-IR irradiation of artery wall suggest that MTT staining and careful examination of H&E-stained tissue sections may be a slightly more sensitive approach to detection of effects on tissues as compared to loss of collagen birefringence in tissue sections. For example, slight increases in staining intensity and slight decreases in thickness of the superficial layer of the artery wall were seen at a fluence of ~72 mJ/mm^2 while in the same tissue no difference in birefringence could be detected with confidence

Heart attack is caused by the clot formation in coronary arteries due to the rupture of vulnerable atherosclerotic plaque (AP) [20]. In the AP of an affected artery, smooth muscle cells migrate to form a fibrous cap that overlays atherogenic matter including lipids, macrophages and foam cells [20]. We observe distinct spectral signatures of the constituents of AP in the 3.2-3.6 μm wavelength window. The mid-IR SC laser based spectroscopy could potentially be used to diagnose atherosclerosis diseases.

Studies of AP with infrared spectroscopy have been reported using Fourier transform infrared spectroscopy (FTIR) based spectroscopy [9,18,19], near-IR reflectance spectroscopy [21], Raman spectroscopy [22], and mid-IR reflection spectroscopy with a synchrotron laser [2]. Compared to the spectroscopic studies of the first overtone features in the near-IR wavelength range, the mid-IR spectral characters of AP compositions not only possess a ~100x enhancement of signal absorbance but also exhibit clear absorption peaks, e.g. ~3420 nm and 3510 nm, which are attributed to the fundamental vibrational modes of the lipid-rich

#106047 - $15.00 USD Received 6 Jan 2009; revised 11 Jun 2009; accepted 23 Jun 2009; published 10 Jul 2009

materials contained in AP [23]. Furthermore, advanced mathematical algorithm, e.g. multivariate data analysis [24], can also be employed to process the mid-IR AP spectral signatures to enhance the diagnosis sensitivity and selectivity. Future study needs to be carried out to evaluate the significance of water and blood absorption in the mid-IR region and their impact on the absorption spectroscopy measurements of the biological targets of interest, e.g. AP compositions [2].

The demonstrated differential damage of adipose tissue versus healthy artery also suggests a potential therapeutic method using the mid-IR SC laser. The laser damage threshold of adipose tissue, which is ~15 mJ/mm^2, is about half of the power required to damage the normal artery, that is ~40 J/mm^2. As pointed out in the previous analysis, the absorbance of laser energy in the mid-IR is considerably higher than that in the near-IR, which results in a reduction of the damage power threshold. Coronary laser angioplasty has been widely studied using optical lasers emitting in a broad range of wavelengths [18], including ultraviolet [25], visible [26], near-IR [13], and mid-IR [12]. While watts of laser power in near-IR (~1-2 μm) can only heat fatty samples above physiological temperature [13], only tens of milliwatts of laser power are required to damage tissue in the 3.2-3.6 μm regime, which is consistent with the results achieved by free electron lasers at 5.75-6.1 μm [12]. Therefore, with the potential dual capability of locating AP and differential damage, treatment might be accomplished in a catheter-based, minimally invasive procedure that might be an add-on to the angiogram (i.e., use the guide wire already in place to insert the mid-IR catheter). The efficacy of the differential damage approach needs to be further studied. The open questions include whether laser damage will cause any significant adverse responses, e.g. inflammation or thrombosis caused by the plaque rupture due to the weakening of the fibrous cap [20]. Further studies must also be conducted to find the optimal laser operation conditions, such as pulse width, energy per pulse, and wavelength band, for both spectroscopic detection and differential damage.

In summary, mid-IR absorption spectra of the structural components of normal artery and AP have been measured by using an all-fiber-integrated SC laser source. Distinctive spectral signatures in 3.2-3.6 μm range that are associated with fatty acids and cholesterol esters absorption are present in the components of AP including foam cells and adipose tissues. On the other hand, endothelial cells, smooth muscle cells and macrophages have a more dominant feature at 2.8-3.2 μm, corresponding to protein and water absorption. Differential damage of the lipid-rich material has been demonstrated by using the SC laser to target the 3.2-3.6 μm fatty acids and cholesterol esters absorption band under laser fluence ranges of ~15-40 mJ/mm^2 for adipose tissue.

Acknowledgements

The authors are grateful to Dr. Hoi-Ying N. Holman at Lawrence Berkeley National Laboratory and Dr. Francis G. Blankenberg at Stanford University Hospital for the fruitful discussion on details of sample preparations and sharing the preprints of the research manuscripts using synchrotron lasers. We sincerely thank Zhao Xu for the help on experimental setup, Dr. Jonathan Eliason for discussion on current medical practices, Dr. Ravi K. Birla for supplying primary human smooth muscle cells, and Dr. Alan J. Hunt for sharing storage and sample preparation facilities at University of Michigan, Ann Arbor. Cryosectioning was performed at the Histology Core Facility at University of Michigan, Ann Arbor with the assistance of Dr. Christopher Strayhorn. Embedding, sectioning and H&E staining of artery wall were conducted by Maria Ripberger in the University of Michigan Center for Organogenesis Morphology Core. Macrophage cell line J774A.1 was obtained from Dr. Katarzyna W. Janczak (Michigan Nanotechnology Institute for Medicine and Biological Sciences). We thank Andy Zakel and Jeremiah Mauricio of Omni Sciences for providing the SC laser prototype picture. This work was supported by the Army Research Office (ARO) under project W911NF-04-C-0078, the Defense Advanced Research Projects Agency (DARPA) under project W31P4Q-05-C-0159, and University of Michigan Cardiovascular Center (CVC) Gelman Innovation/Innovator Grant. The University of

#106047 - $15.00 USD Received 6 Jan 2009; revised 11 Jun 2009; accepted 23 Jun 2009; published 10 Jul 2009

Michigan is partially funded through sub-contracts from Omni Sciences, Inc. Prof. Mohammed N. Islam is also the Founder and Chief Technology Officer of Omni Sciences, Inc.

#106047 - $15.00 USD Received 6 Jan 2009; revised 11 Jun 2009; accepted 23 Jun 2009; published 10 Jul 2009